

- (28) Hlavacek, B.; Sangster, J. *Can. J. Chem. Eng.* **1976**, *54*, 115.
- (29) Jellinek, H. H. G. *Water Structure at the Water-Polymer Interface*; Plenum Press: New York, 1972.
- (30) Franks, F., Ed. *Water, A Comprehensive Treatise*; Plenum Press: New York, 1975; Vol. 4.
- (31) Tanford, C. *The Hydrophobic Effect, Formation of Micelles and Biological Membranes*; Wiley: New York, 1973.
- (32) Bagatskii, N. A.; Svintsitskii, N. I.; Pas'ko, S. P.; Uskov, I. A.; Zelenev, Yu. V. *Polym. Sci. USSR (Engl. Transl.)* **1986**, *28* (8), 1846.
- (33) Ben-Naim, A. *Water and Aqueous Solutions*; Plenum Press: New York, 1975.
- (34) Hoy and Hoy, U.S. Patent 4,209,605, 1980.
- (35) Molyneux, P. *Water Soluble Synthetic Polymers: Properties and Behavior*; CRC Press: Boca Raton, FL, 1983, Vol. II, p 18.
- (36) McCormick, C. L.; Salazar, L. C. *PMSE* **1987**, *57*, 859.
- (37) Morgan, S. E. Ph.D. Dissertation, University of Southern Mississippi, 1988.
- (38) McCormick, C. L.; Johnson, C. B. *Macromolecules* **1988**, *21*, 686.
- (39) McCormick, C. L.; Johnson, C. B. *Macromolecules* **1988**, *21*, 694.
- (40) Schlichting, H. *Boundary Layer Theory*; McGraw-Hill: New York, 1979; p 647.
- (41) Bird, R. B.; Stewart, W. E.; Lightfoot, E. N. *Transport Phenomena*; Wiley: New York, 1960; p 181.
- (42) Blackmon, K. P. Ph.D. Dissertation, University of Southern Mississippi, 1986.
- (43) McCormick, C. L.; Hutchinson, B. H.; Morgan, S. E. *Makromol. Chem.* **1987**, *188*, 357.
- (44) Schick, M. J. *J. Phys. Chem.* **1964**, *68* (12), 3585.
- (45) Mukerjee, P.; Ray, A. J. *J. Phys. Chem.* **1963**, *67*, 190.
- (46) Bandrup, J.; Immergut, E. H., Eds. *Polymer Handbook*, 2nd ed.; Wiley: New York, 1975.
- (47) Pecora, R.; Berne, B. *Dynamic Light Scattering*; Wiley: New York, 1976.
- (48) Flory, P. J. *Principles of Polymer Chemistry*; Cornell University Press: London, 1953.

**Registry No.** (NaAMB)(PAM) (copolymer), 100047-18-5; NaAMB 100 (homopolymer), 40404-89-5; DAAM (copolymer), 25231-54-3; ADASAM (copolymer), 125847-98-5; ADAS (copolymer), 125847-99-6.

## High-Resolution Solid-State Carbon-13 Nuclear Magnetic Resonance Study of Polybenzimidazole/Polyimide Blends

Janusz Grobelny,<sup>†</sup> David M. Rice, Frank E. Karasz,\* and William J. MacKnight

Department of Polymer Science and Engineering, University of Massachusetts, Amherst, Massachusetts 01003. Received August 25, 1989;  
Revised Manuscript Received October 31, 1989

**ABSTRACT:** Miscible blends of polybenzimidazole with an aromatic polyimide and a polyetherimide have been studied by high-resolution <sup>13</sup>C CPMAS NMR in the solid state. The observed resonance signals in the spectra of individual components of the blends have been assigned, and these assignments have been supported by interrupted decoupling experiments. The blending of PBI with polyimide induces a broadening and a downfield shift of the aromatic polyimide phthalimide carbonyl resonance with respect to that of the pure material. This difference between the spectra of the blends and those of the respective mechanical mixtures has been interpreted to be the result of the formation of specific hydrogen bonds between the PBI imidazole amine function and the polyimide phthalimide carbonyl function. Miscibility in the blend of PBI with the aromatic polyimide has also been confirmed by a study of the proton rotating frame spin-lattice relaxation behavior.

### Introduction

A new class of high-performance, miscible binary blends of polybenzimidazoles (PBI) with several aromatic polyimides (PI) has recently been described.<sup>1</sup> Miscibility in these blends over a wide range of compositions has been demonstrated by differential scanning calorimetry as well as by dynamic mechanical analysis.<sup>1,2</sup> Infrared spectroscopic studies of these PBI/PI systems have indicated that miscibility in these polymers is related to a specific interaction involving the phthalimide carbonyl groups of polyimide and imidazolic amine groups of PBI.<sup>3,4</sup>

The aim of the present work has been to obtain evidence for miscibility and interchain interaction in PBI/PI binary blends by means of high-resolution solid-state <sup>13</sup>C CPMAS NMR.<sup>5</sup> A strong interaction between blend components such as hydrogen bonding should cause changes in the <sup>13</sup>C chemical shifts of those resonances

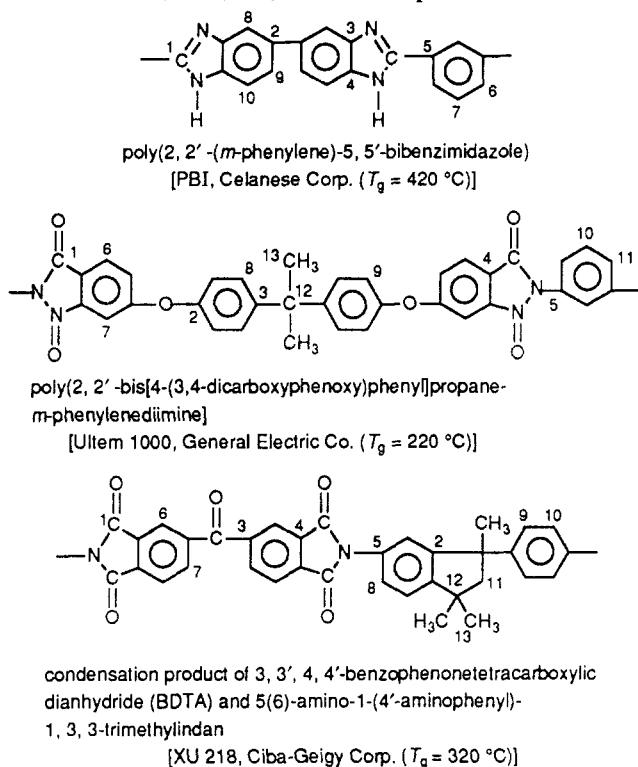
involved in the interaction, in this case the phthalimide carbonyl with the bibenzimidazole amine. We report here composition dependent changes in the <sup>13</sup>C CPMAS line shape of the phthalimide carbonyl in blends with PBI and show that these changes are consistent with hydrogen bonding between the blend constituents. In addition, <sup>13</sup>C CPMAS NMR has been used to study proton spin diffusion in these blends,<sup>6-10</sup> and evidence for miscibility was obtained from an equality of the values of the proton rotating frame spin-lattice relaxation time  $T_{1\rho}^H$  for the two blend components.

### Experimental Section

The following polymers were used in the study: poly(2,2'-(*m*-phenylene)-5,5'-bibenzimidazole) [PBI, Celanese Corp. ( $T_g = 420^\circ\text{C}$ )], poly[2,2'-bis[4-(3,4-dicarboxyphenoxy)phenyl]propane-*m*-phenylenedimine] [Utem 1000, General Electric Co. ( $T_g = 220^\circ\text{C}$ )], and the condensation product of 3,3',4,4'-benzophenonetetracarboxylic dianhydride and 5(6)-amino-1-(4'-aminophenyl)-1,3,3'-trimethylindan [XU 218, Ciba-Geigy Corp. ( $T_g = 320^\circ\text{C}$ )]. Chart I lists the structures. These polymers

<sup>†</sup> Permanent address: Institute of Polymer Chemistry, Polish Academy of Sciences, 41-800 Zabrze, Poland.

Chart I  
Structures and Codes of Compounds Used<sup>a</sup>



<sup>a</sup> The numbers on the structures correspond to the chemical shifts in Figures 1 and 2.

were purified by precipitation into methanol from 3% (w/v) solutions in *N,N*-dimethylacetamide (DMAc) and were vacuum dried at  $200^\circ\text{C}$  for several days.

Miscible blends of PBI/Ultem 1000 and PBI/XU 218 in powder form were prepared by mixing 3% (w/v) DMAc solutions of the required materials in the desired composition ratios and precipitating into methanol; these solutions yielded blends in the form of fine powders. The powders were then filtered, washed with water, and dried under vacuum at  $200^\circ\text{C}$ .

Mechanical mixtures were prepared by physically mixing the powders of the individual blend components. The pure components had been previously precipitated with MeOH from DMAc, as described for blends. Miscible blends of PBI/Ultem 1000 and PBI/XU 218 were also cast as films according to the methods of Guerra et al.<sup>3</sup> and Musto et al.<sup>4</sup> <sup>13</sup>C CPMAS line shapes obtained from the films were similar to those of powders.

The content of residual DMAc in the blends and in the pure blend constituents did not exceed 1 wt %, as revealed by thermogravimetric analysis. The blends were shown by DSC to have single, composition-dependent glass transitions,  $T_g$ , lying between those of the constituent polymers.<sup>1</sup>

The blends were annealed in a nitrogen atmosphere for 5 min above their reported phase separation temperatures.<sup>2</sup> For a 50/50 wt % PBI/Ultem 1000 blend the annealing temperature was  $350^\circ\text{C}$ , whereas a 75/25 wt % blend of the two polymers was annealed at  $400^\circ\text{C}$ . For the case of the PBI/XU 218 blends the annealing temperatures were  $430$  and  $450^\circ\text{C}$  for 50/50 and 75/25 wt % compositions, respectively.

High-resolution solid-state <sup>13</sup>C CPMAS NMR spectra were obtained at ambient temperature with an IBM AF-200 spectrometer operating at a <sup>13</sup>C resonance frequency of 50.3 MHz and a Bruker MSL-300 at 75.5 MHz. Hartmann-Hahn spin lock cross polarization along with magic angle sample spinning (CPMAS) were used to obtain <sup>13</sup>C spectra from the solid state.<sup>5,11,12</sup> In the present study the matched spin lock CP transfer employed <sup>13</sup>C and <sup>1</sup>H magnetic fields of 50 kHz (75 kHz for the MSL-300). Proton decoupling was provided at the same strength as the spin locking field. The sample spinning at magic angle was carried out at rates between 3500 and 5000 Hz for both instruments. Samples of about 200 mg were hand-com-

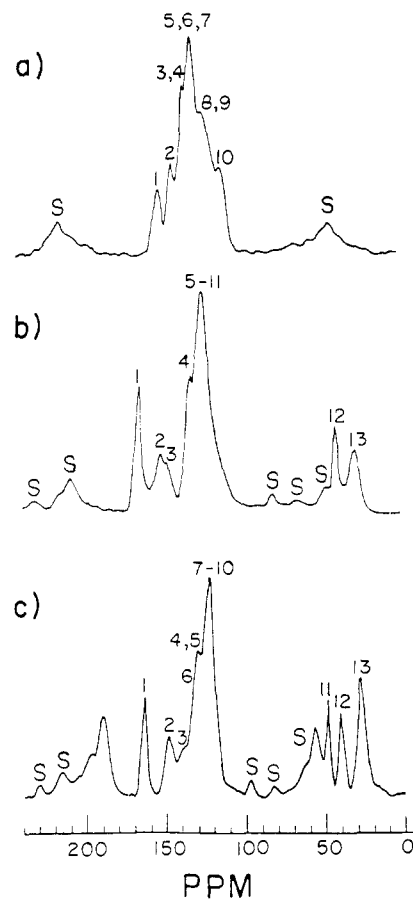


Figure 1. <sup>13</sup>C CPMAS NMR spectra of (a) PBI, (b) Ultem 1000, and (c) XU 218; (1.5-ms contact time; the spinning sidebands are denoted by S). The numbers on the peaks correspond to those on the structures shown in Chart I.

pacted into sapphire rotors with KelF end caps. For all the polymers 600–1000 scans were accumulated with a 3-s delay between pulse sequence repetitions. Chemical shifts were referenced relative to tetramethylsilane, TMS.

An interrupted decoupling experiment<sup>13</sup> was also used for <sup>13</sup>C assignment. For this experiment a short delay (typically 50–100  $\mu\text{s}$ ) was inserted in a <sup>13</sup>C CPMAS sequence between carbon <sup>13</sup>C–<sup>1</sup>H proton contact and the data acquisition. The values of <sup>1</sup>H–<sup>1</sup>H spin-lattice relaxation time in the rotating frame  $T_{1\rho}^H$  were measured from analysis of the changes in the carbon magnetization for long contact times.<sup>6</sup>

Line fitting was carried out with the Bruker MSL-300 using software supplied by the manufacturer.

## Results and Discussion

<sup>13</sup>C CPMAS NMR Assignment of PBI, Ultem 1000, and XU 218. The <sup>13</sup>C CPMAS NMR spectra of the pure blend components PBI, Ultem 1000, and XU 218 are shown in Figure 1. Chemical shift assignments are displayed in Table I. The spectrum of PBI (Figure 1, curve a) consists of several lines that can be identified in order of increasing magnetic field as lines arising from the carbons of imidazole rings attached to phenylene rings (151 ppm), the carbons connecting benzimidazole rings in the bibenzimidazole system (142 ppm), and the aromatic carbons bound to the nitrogen atoms (134 ppm). The three remaining lines (129, 120, and 111 ppm) have been assigned to the protonated carbons of PBI with a contribution from the nonprotonated carbons of the phenylene ring to the line centered at 129 ppm.

The assignment of resonance signals has been supported by the application of an interrupted decoupling pulse sequence and a short contact time pulse sequence

**Table I**  
<sup>13</sup>C Chemical Shifts of PBI, Ultem 1000, and XU 218 in the Solid State (ppm from TMS)

PBI		PI Ultem 1000		PI XU 218	
chem shift	carbon <sup>a</sup>	chem shift	carbon <sup>a</sup>	chem shift	carbon <sup>a</sup>
				~200	benzophenone carbonyl
151	1	165	1	165	1
142	2	151	2	150	2
134	3,4	147	3	140	3
129	5,6,7	133	4	133	6
120	8,9	124	5-11	130	4,5
111	10			124	7-10
				50	11
		42	12	42	12
		31	13	30	13

<sup>a</sup> See the structures shown in Chart I for carbon numbers.

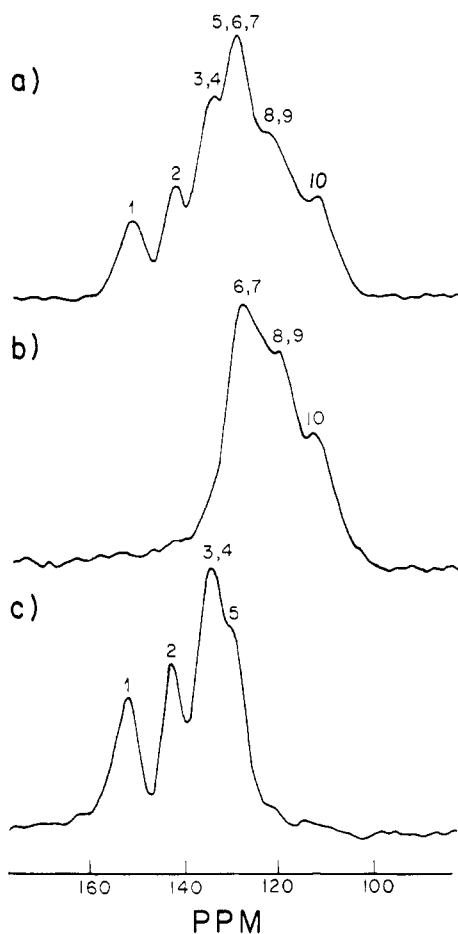


**Figure 2.** <sup>13</sup>C CPMAS NMR spectra of PBI: (a) 1.5-ms contact time; (b) 0.02-ms contact time; (c) 90-μs interrupted decoupling with 1.5-ms contact time. The numbers on the peaks correspond to those on the structures shown in Chart I.

that can distinguish protonated carbons (with strong dipolar <sup>13</sup>C-<sup>1</sup>H couplings) from nonprotonated carbons with weak coupling.<sup>13</sup> These spectra are shown in Figure 2 for PBI. In the spectrum shown in Figure 2, curve b, obtained for short (20 μs) contact time, only the lines at 129, 120, and 111 ppm, assigned to the protonated carbons, are present. In contrast, in the interrupted decoupling experiment, the magnetization of protonated carbons dephases due to a strong <sup>13</sup>C-<sup>1</sup>H dipolar interaction, allowing the signals of carbons without directly attached protons to be selectively observed. The result of such an approach with a 90-μs delay is shown in Figure 2, curve c. The signal of the nonprotonated carbons of the meta-substituted/phenylene ring can be resolved

in Figure 2, curve c, as a higher field shoulder of the 134 ppm peak.

Figure 1, curve b, presents the <sup>13</sup>C CPMAS NMR spectrum of the Ultem 1000 poly(ether imide). The lowest field line at 165 ppm can be assigned to the imide carbonyl carbons due to the electron-withdrawing effect of the oxygen. The three other lines at 151, 147, and 133 ppm, respectively, are the aromatic carbons bonded to ether oxygens, aromatic carbons attached to quaternary aliphatic carbons, and the remaining nonprotonated carbons of the phthalimide rings. All the remaining protonated aromatic carbons and N-linked *m*-phenylene carbons give rise to the broad resonance with a maximum at 124 ppm. The quaternary aliphatic carbon resonance appears at 42 ppm, and the methyl carbon signal appears at 31 ppm.

Support for this assignment was also obtained by using the selective pulse sequences described previously (spectra are not shown). A short contact time <sup>13</sup>C CPMAS experiment permitted the exclusive observation of protonated carbons at 124 ppm, whereas with the 90-μs interrupted decoupling, the nonprotonated carbons at 151, 147, and 133 ppm are evident. The methyl carbon signal does not vanish because of very weak coupling of the protons due to fast rotation.<sup>13</sup> The interrupted decoupling experiment enabled the signal of the aromatic carbons directly bonded to the imide nitrogens to be detected separately at 124 ppm.

Figure 1, curve c, shows the <sup>13</sup>C CPMAS spectrum of the XU 218 polyimide. The appearance of spinning sidebands in the vicinity of 200 ppm obscures the resonance of the benzophenone carbonyl carbon at its usual position of 196 ppm.<sup>14</sup> The imide carbonyl carbons absorb at 165 ppm, as in the case of the Ultem 1000 poly(ether imide), but the signal of the aromatic carbons attached to imide carbonyl groups (130 ppm) is shifted 3 ppm upfield relative to the position of the corresponding carbon signal of Ultem 1000. The evidence for this assignment was obtained from a short contact cross polarization experiment, and the short contact time reveals two lines at 133 and 124 ppm that can be assigned respectively to the protonated carbons located in the ortho position relative to both kinds of carbonyl groups (strong mesomeric effect of electron-attracting substituents) and to the remaining protonated aromatic carbons.<sup>14</sup>

The nonprotonated aromatic carbons connected to aliphatic carbons give rise to the line at 150 ppm, and the carbons bonded to the benzophenone carbonyl are at 140 ppm. The aromatic carbons linked with nitrogen must contribute to the line at 130 ppm. This line is not seen as a separate peak in the 90-μs interrupted decoupling spectrum, in contrast to the situation observed for the Ultem 1000 poly(ether imide). Aliphatic carbons give rise to resonances at 50 (methylene group), 42 (quaternary), and 30 ppm (methyl groups). The signals of the methyl and methylene carbons remain in the interrupted decoupling spectrum, indicating mobility in the aliphatic part of the XU 218 structure.

**<sup>13</sup>C CPMAS Spectra of PBI/Ultem 1000 and PBI/XU 218 Blends.** Figures 3-5 display <sup>13</sup>C CPMAS NMR spectra of PBI/Ultem 1000 and PBI/XU 218 blends. For comparison, in each figure the spectrum of the mechanical mixture of the respective polymer pair is shown with a dotted line. This display of the spectra reveals changes in the line shape due to blending and shows changes in the isotropic chemical shifts that could be a result of specific molecular interactions between blend components. Changes in the isotropic chemical shift originate from

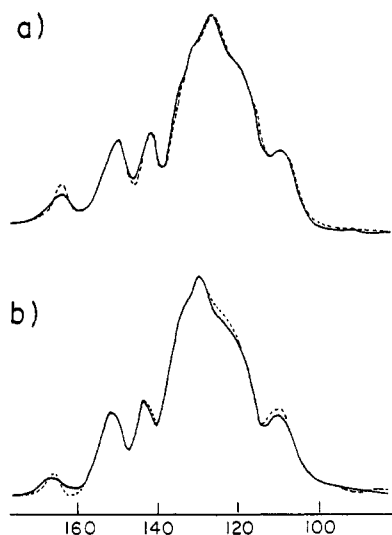


**Figure 3.** (a)  $^{13}\text{C}$  CPMAS NMR spectra of (—) 75/25 wt % PBI/Utem 1000 blend and (---) 75/25 wt % PBI/Utem 1000 mechanical mixture. (b)  $^{13}\text{C}$  CPMAS NMR spectra of (—) 75/25 wt % PBI/XU 218 blend and (---) 75/25 wt % PBI/XU 218 mechanical mixture. Both spectra were obtained with a 1.5-ms contact time and a 4-kHz spinning rate.

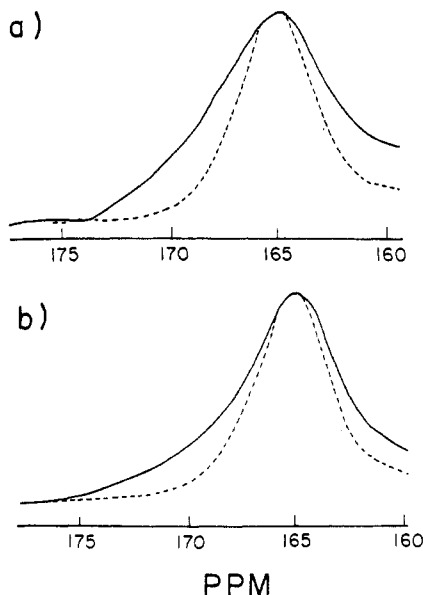


**Figure 4.**  $^{13}\text{C}$  CPMAS NMR spectra of the Utem 1000 carbonyl resonance of PBI/Utem 1000 blends: (a) 75/25 wt % blend (—) and 75/25 wt % mechanical mixture (---); (b) 50/50 wt % blend (—) and 50/50 wt % mechanical mixture (---).

relatively short-range effects, so they necessarily indicate interaction between the blend constituents on a molecular level. Chemical shift changes may be induced directly by interchain shielding, that is by alteration of the carbon electron cloud by a change in chemical environment, or indirectly by changes in conformation through modification of bond angles and variations in intrachain nearest-neighbor distances.<sup>15</sup> The spectral changes displayed in Figures 3–5 provide strong evidence for intimate intermixing on a molecular scale.

Figure 3 shows the  $^{13}\text{C}$  spectra of the blends of PBI with the Utem 1000 poly(ether imide) and with the XU 218 polyimide. Figure 3, curve a, shows the spectrum of a 75/25 wt % PBI/Utem 1000 blend, and Figure 3, curve b, shows the spectrum of a 75/25 wt % PBI/XU 218 blend. In both spectra, the corresponding spectrum of the mechanical mixture is superimposed as a dotted line. One can see that for both blends that the greatest dif-

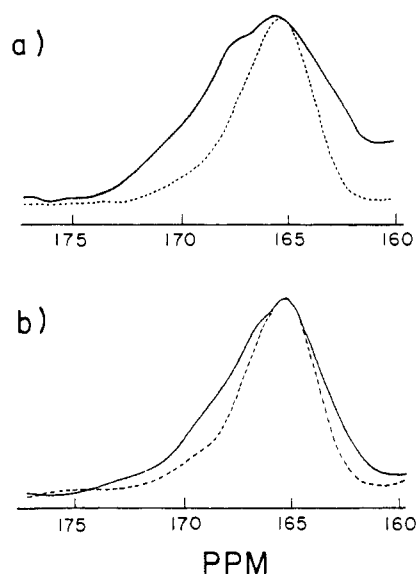


**Figure 5.**  $^{13}\text{C}$  CPMAS NMR spectra of the XU 218 carbonyl resonance of PBI/XU 218 blends: (a) 75/25 wt % blend (—) and 75/25 wt % mechanical mixture (---); (b) 50/50 wt % blend (—) and 50/50 wt % mechanical mixture (---).

ference between the spectra of the blend and the mixture occurs for the carbonyl resonance at 165 ppm. The spectra of the blend and mechanical mixture also deviate at other chemical shifts, but the difference is small compared to the line intensity. These other differences also occur in regions where the spectra of PBI and polyimide overlap, and so no effort has been made to determine their origin.

The 165 ppm line arising from the carbonyl carbons of either the Utem 1000 or the XU 218 polyimide is well resolved in all blend spectra. The study of this particular resonance may provide information about intermolecular interactions in PBI/PI systems. The presence of PBI in a blend decreases the intensity and causes broadening of the polyimide carbonyl resonance. The broadening of the carbonyl resonance is greater toward higher parts per million values and becomes more pronounced as the content of PBI increases in the blends.

Figure 4 shows an enlargement of the imide carbonyl chemical shift region for two blend compositions of PBI and Utem 1000. Figure 4, curve a, shows a spectrum of a 75/25 wt % PBI/Utem 1000 blend, and Figure 4, curve b, shows a spectrum of a 50/50 wt % blend. The spectrum of the respective mechanical mixtures (dotted lines) have been included for comparison. In the imide carbonyl region, only Utem 1000 contributes to the spectrum, and the spectrum of the mechanical mixture is similar to that of the pure polyimide. The spectra of the blend and the mixture have been normalized to the same height to emphasize differences in the line shape. Figure 4 shows the increase in the carbonyl line width and indicates that the increase occurs preferentially in the downfield direction (greater parts per million). The spectrum of the 75/25 wt % blend also shows some structure and appears to consist of at least three superimposed lines with centers at 172 ppm, 168 ppm and 165 ppm.

Figure 5 is an enlargement, similar to Figure 4, of the imide carbonyl chemical shift region of the PBI/XU 218 blend. Figure 5, curve a, is the 75/25 wt % blend; Figure 5, curve b, is the 50/50 wt % blend, and the spectra of the mechanical mixtures are shown for comparison (dotted lines). The spectra of PBI/XU 218 blends are similar to those of the PBI/Utem 1000 blends. The spectrum of the 75/25 wt % PBI/XU 218 blend also shows

structure and appears to consist of three lines with shifts of 172, 168, and 165 ppm. The 50/50 wt % blend shows structure as well, although the intensities of the downfield lines are smaller.

Blends of PBI and either Ultem 1000 or XU 218 are known to undergo irreversible phase separation at temperatures above that of the respective blend glass transition.<sup>4</sup> Samples of both blends have been annealed at temperatures sufficient to induce phase separation, and the resulting spectra of the phase-separated blends are similar to those of the respective mechanical mixtures.

It is well-known that the resonance of a carbonyl group in a solvent capable of hydrogen bonding is found at higher parts per million values than a similar resonance in a nonpolar solvent. For example, the carbonyl resonance of acetone in a polar solvent such as water is 11.5 ppm downfield from its position in a nonpolar solvent such as cyclohexane. The shift has been attributed directly to the hydrogen-bonding interaction of the solvent pair.<sup>16</sup> Similar behavior should also be expected to occur in a miscible mixture of two amorphous polymers where hydrogen bonding is present. The principal difference between the two systems is in the rate of molecular motion. The  $^{13}\text{C}$  chemical shift of carbonyl in a liquid mixture is a time average of all the possible arrangements of coordinating molecules, including those arrangements that involve hydrogen bonding. In a glassy solid mixture of PBI and polyimide, steric constraints prevent most of the molecular motion, and one should expect a distribution of chemical shifts rather than a single average.<sup>17</sup> For those particular arrangements of the two polymer chains that involve specific hydrogen bonding, the carbonyl resonance should be shifted downfield. We suggest that the shifted resonances in Figures 4 and 5 can be attributed to that fraction of the polyimide carbonyls that are involved in hydrogen bonds with the PBI amine group.

The  $^{13}\text{C}$  CPMAS results presented here can be directly compared with Fourier transform infrared spectroscopic (FTIR) results obtained with similar blends.<sup>3,4</sup> Blending of PBI is known to cause a composition-dependent shift of the phthalimide carbonyl stretching vibration of XU 218 from 1727  $\text{cm}^{-1}$  for pure XU 218 to 1720  $\text{cm}^{-1}$  for an 80/20 wt % PBI/XU 218 blend; the effect on Ultem 1000 is similar. In addition, the N-H stretching band of PBI at 3420  $\text{cm}^{-1}$  is also altered in the blends. As with the NMR data, high-temperature annealing appears to reverse the shift and this effect is now under study by FTIR methods.<sup>3</sup> Because thin films are typically used for infrared spectroscopy, the spectra in Figures 3-5 have been obtained by using similar films.

The carbonyl  $^{13}\text{C}$  CPMAS NMR line shape is composed of a distribution of NMR lines of different chemical shifts, for which the intrinsic width of each line in the absence of molecular motion is narrow. Therefore the carbonyl NMR line shape directly reveals the distribution of chemical shifts and the molecular environments that affect the chemical shift. This line shape must be composed of contributions from free carbonyl groups as well as those that are affected by hydrogen bonding. Similarly the band shape of the infrared carbonyl is the result of a distribution of molecular force constants for vibration, and it is well-known that hydrogen bonding causes a shift of the carbonyl stretch frequency to lower wavenumbers. The carbonyl infrared band shape also reveals the distribution of molecular environments resulting from hydrogen bonding, and infrared data can be analyzed to calculate the population of hydrogen-bonded carbonyl groups.<sup>18,19</sup> Both NMR and infrared data should

be directly comparable, and it should be possible to fit both sets of data simultaneously with an appropriate model for hydrogen bonding.

The phthalimide infrared band shape of Ultem 1000 in PBI has been resolved into two bands by line fitting, the first band similar to pure polyimide and the second band due to polyimide involved in interactions with PBI.<sup>19</sup> In blends containing excess PBI it has been found that only 50% of the phthalimide intensity is altered. It has been concluded that only 50% of the phthalimide groups are involved in hydrogen bonds with PBI.

The carbonyl NMR line shapes of Figures 4 and 5 can be analyzed in a manner similar to that for the infrared data. The downfield carbonyl NMR resonance intensity has been attributed to hydrogen bonding with PBI. One can determine the fraction of shifted resonance intensity by simulation of the spectra in Figures 4 and 5 with a two-line model similar to the model used for infrared spectroscopy. The first component should have a line shape similar to that of pure polyimide, and the second component should account for resonances shifted downfield through interaction with PBI. For the PBI/Ultem 1000 blends, 15% (50/50 wt %) to 30% (75/25 wt %) of the carbonyl intensity is shifted downfield. For the PBI/XU 218 blends, 20% (50/50 wt %) to 40% (75/25 wt %) of the carbonyl intensity is shifted downfield. These percentages are in approximate agreement with those indicated by infrared data. A more exact comparison of percentages would require a model for the PBI-polyimide interaction, but it is clear from both sets of data that a fraction of the polyimide segments interacts with PBI and that in blends with excess PBI a fraction of polyimide segments also remains unperturbed by blending.

**Measurement of the  $T_{1\rho}^H$  of PBI/Polyimide Blends.** In polymer blends the values of the proton rotating frame spin-lattice relaxation time,  $T_{1\rho}^H$ , are influenced by the efficiency of spin diffusion among protons of the constituent polymers. This efficiency, in turn, is dependent upon short-range spatial proximity of chemically different chains. In a miscible binary blend, the protons of the two components are closely coupled and relax with a common rate through the spin-diffusion mechanism. The examination of the  $T_{1\rho}^H$  values provides information about the homogeneity of blends on a molecular scale, and this approach is considered to be an NMR criterion for miscibility in blend systems.<sup>6</sup>

The value of the  $T_{1\rho}^H$  for these blends has been determined from a plot of the  $^{13}\text{C}$  CPMAS resonance intensity versus cross polarization contact time (Figure 6). After an initial buildup of carbon polarization at short contact times, the carbon signal intensity decays in concert with the proton magnetization with a time constant equal to the  $T_{1\rho}^H$ . The final slope of a plot of the logarithm of intensity versus contact time will yield the value of the  $T_{1\rho}^H$ . Table II shows a compilation of these values for the various carbon resonances of PBI, polyimides, and the blends. It can be seen that, as expected, the values of  $T_{1\rho}^H$  for a single blend component are similar and the variation in the  $T_{1\rho}^H$  for the various carbon lines was  $\pm 5\%$ . The average value of  $T_{1\rho}^H$  for PBI was 9 ms, for Ultem 1000 was 10.5 ms, and for XU 218 was 14.5 ms. The carbonyl function of pure XU 218 possessed an anomalously long  $T_{1\rho}^H$  of 17 ms.

For the two 50/50 wt % blends, the value of  $T_{1\rho}^H$  was measured for each distinguishable line in the spectrum. These included the aliphatic methyl resonances of polyimide (32, 42 ppm), the phthalimide carbonyl resonance of polyimide (165 ppm), and the ring protons of PBI (111

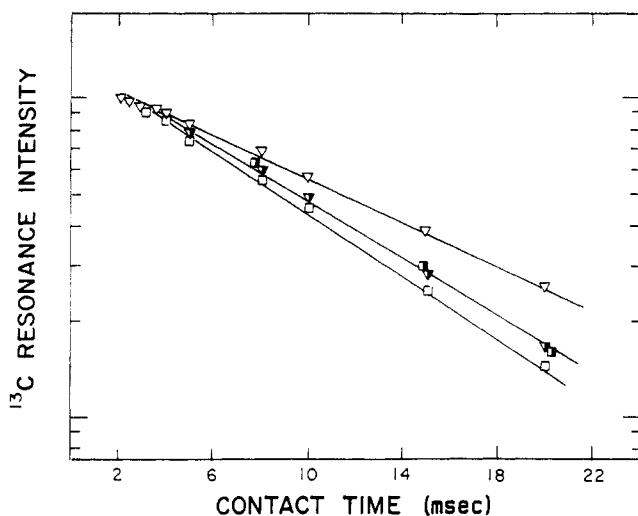


**Figure 6.** Variation of carbon magnetization versus cross polarization contact time for PBI ( $\square$ ), XU 218 ( $\nabla$ ), and 50/50 wt% PBI/XU 218 blend ( $\blacksquare$ ,  $\blacktriangledown$ ). The squares refer to the PBI relaxation at 111 ppm, the triangles refer to XU 218 relaxation at 30 ppm, and the half-filled symbols refer to these resonances in the blend.

**Table II**  
Proton Spin-Lattice Relaxation Times in the Rotating Frame  $T_{1\rho}^H$  (ms) of PBI, Ultem 1000, XU 218, and 50/50 wt % Blends of PBI with Ultem 1000 and with XU 218

XU 218		PBI/XU 218 <sup>a</sup>		PBI		PBI/Ultem 1000 <sup>a</sup>		Ultem 1000	
obsd peak, ppm	$T_{1\rho}^H$	obsd peak, ppm	$T_{1\rho}^H$	obsd peak, ppm	$T_{1\rho}^H$	obsd peak, ppm	$T_{1\rho}^H$	obsd peak, ppm	$T_{1\rho}^H$
165	17.0			151	8.7			165	11.3
				142	8.9				
130	14.5			129	9.5			133	10.5
124	14.0			120	8.7			124	11.0
		111	9.8	111	9.2	111	9		
50	14.2	50	9.5						
42	14.4	42	9.8			42	10	42	11.3
30	14.2	30	10			31	8.7	31	10

<sup>a</sup> 50/50 wt %.

ppm). It can be seen from Table II that the values of  $T_{1\rho}^H$  for the blend samples are indeed between those of the pure components and can be predicted by a model for linear additivity of relaxation rates.<sup>20</sup> For the PBI/XU 218 blend, the value of  $T_{1\rho}^H$  for polyimide changes significantly, from 14.5 to 10.5 ms, and the value of  $T_{1\rho}^H$  measured from PBI changes from 9 to 10 ms. For the PBI/Ultem 1000 blend the values of  $T_{1\rho}^H$  for the two pure components are similar. The PBI/Ultem 1000 results are thus consistent with miscibility but do not provide positive evidence.

## Conclusions

Results from  $^{13}\text{C}$  CPMAS NMR of the two PBI/polyimide blends provide evidence for miscibility and, for these systems, support the conclusion that specific hydrogen bonds exist between the phthalimide carbonyl of polyimide and the imidazolic amine bond of PBI. Evidence for this hydrogen bonding comes from a change in the carbonyl spectral line shape of polyimide. Addition of PBI broadens this resonance, principally in the downfield direction, and a downfield carbonyl chemical shift indicates the existence of a fraction of carbonyl to amine

hydrogen bonds. PBI/polyimide blends are amorphous, and only a fraction of the carbonyls should undergo hydrogen bonding; NMR results show that only a fraction of the carbonyl resonances are shifted downfield. NMR results are in agreement with FTIR results, which also indicate hydrogen bonding. The extent of hydrogen bonding indicated by the two methods is similar.

Evidence for miscibility in the 75/25 wt % PBI/XU 218 blend is also obtained from the measurement of  $T_{1\rho}^H$ . The values of  $T_{1\rho}^H$  for the PBI and Ultem 1000 are similar so no positive conclusions can be drawn for the PBI/Ultem 1000 blend.

We have shown that when the interaction between polymers is strong, as with hydrogen bonding, one should not overlook the NMR data available from simple changes in the  $^{13}\text{C}$  CPMAS chemical shift. Hydrogen bonding in polymer blends has been studied extensively by FTIR methods,<sup>20</sup> and one should note that the spectral resolution of a  $^{13}\text{C}$  CPMAS spectrum is not very different from that of an FTIR spectrum. These two independent methods can provide complementary data of about the same precision, and so, at least for studies of hydrogen bonding, NMR spectra should be compared with infrared spectra of polymer blends.

**Acknowledgment.** We are indebted to Dr. L. Charles Dickinson and Dr. G. Smyth for helpful NMR discussions and Dr. Pellegrino Musto for discussion of his infrared data for these blends. This research was supported by the Advanced Research Projects Agency of the Department of Defense (Contract No. F49620-85-0127) and the U.R.I. NMR Laboratory.

## References and Notes

- Leung, L.; Williams, D. J.; Karasz, F. E.; MacKnight, W. J. *Polym. Bull.* **1986**, *16*, 457.
- Choe, S.; MacKnight, W. J.; Karasz, F. E. In *Polyimides*; Feger, C., Ed.; Elsevier: Amsterdam, 1989.
- Musto, P.; Karasz, F. E.; MacKnight, W. J. *Polymer* **1989**, *30*, 1012.
- Guerra, G.; Choe, S.; Williams, D. J.; Karasz, F. E.; MacKnight, W. J. *Macromolecules* **1981**, *21*, 231.
- Havens, J. R.; Koenig, J. L. *Appl. Spectrosc.* **1983**, *37*, 226.
- Stejskal, E. O.; Schaefer, J.; Sefcik, M. D.; McKay, R. A. *Macromolecules* **1981**, *14*, 275.
- Dickinson, L. C.; Yang, H.; Chu, C.-W.; Stein, R. S.; Chien, J. C. W. *Macromolecules* **1987**, *20*, 1757.
- Schaefer, J.; Sefcik, M. D.; Stejskal, E. O.; McKay, R. A. *Macromolecules* **1981**, *14*, 188.
- Tekely, P.; Laupretre, F.; Monnerie, L. *Polymer* **1985**, *26*, 1081.
- Gobbi, G. C.; Silvestri, R.; Russell, T. P.; Lyster, J. R.; Fleming, W. W.; Nishi, T. *J. Polym. Sci., Polym. Lett.* **1987**, *25*, 61.
- Lyster, J. R.; Yannoni, C. S. *IBM J. Res. Dev.* **1983**, *27*, 302.
- Laupretre, F.; Monnerie, L.; Block, B. *Anal. Chim. Acta* **1986**, *189*, 117.
- Opella, S. J.; Frey, M. H. *J. Am. Chem. Soc.* **1979**, *101*, 5854.
- Havens, J. R.; Ishida, H.; Koenig, J. L. *Macromolecules* **1981**, *14*, 1327.
- Vanderhart, D. L.; Earl, W. L.; Garroway, A. M. *J. Magn. Reson.* **1981**, *44*, 361.
- Maciel, G. E.; Ruben, G. C. *J. Am. Chem. Soc.* **1963**, *85*, 3903.
- Komoroski, R. A.; Mandelkern, L. In *High Resolution NMR Spectroscopy of Synthetic Polymers in Bulk*; Komoroski, R. A., Ed.; VCH: New York, 1986; p 4.
- Coleman, M. M.; Skrovonek, D. J.; Hu, J.; Painter, P. C. *Polym. Prepr. (Am. Chem. Soc., Div. Polym. Chem.)* **1987**, *28*, 19.
- Musto, P.; Karasz, F. E.; MacKnight, W. J., submitted for publication in *Macromolecules*.
- Douglass, D. C. In *Polymer Characterization by ESR and NMR*; Woodward, A. E.; Bovey, F. A., Eds.; ACS Symposium Series 142; American Chemical Society: Washington, D.C., 1980.